THE JOURNAL OF PHYSICAL CHEMISTRY Letters

LETTER

pubs.acs.org/JPCL

When a Metastable Oxide Stabilizes at the Nanoscale: Wurtzite CoO Formation upon Dealloying of PtCo Nanoparticles

Vasiliki Papaefthimiou,[†] Thierry Dintzer,[†] Véronique Dupuis,[‡] Alexandre Tamion,[‡] Florent Tournus,[‡] Detre Teschner,[§] Michael Hävecker,[§] Axel Knop-Gericke,[§] Robert Schlögl,[§] and Spiros Zafeiratos*[,†]

[†]Laboratoire LMSPC, UMR7515 CNRS-Université de Strasbourg, 25 rue Becquerel, 67087 Strasbourg, France

[‡]Laboratoire PMCN UMR 5586, University Lyon 1, CNRS, F-69622 Villeurbanne cedex, France

[§]Fritz-Haber-Institut der Max-Planck-Gesellschaft, Faradayweg 4-6, 14195 Berlin, Germany

Supporting Information

ABSTRACT: Ambient pressure photoelectron and absorption spectroscopies were applied under 0.2 mbar of O_2 and H_2 to establish an unequivocal correlation between the surface oxidation state of extended and nanosized PtCo alloys and the gas-phase environment. Fundamental differences in the electronic structure and reactivity of segregated cobalt oxides were associated with surface stabilization of metastable wurtzite-CoO. In addition, the promotion effect of Pt in the reduction of cobalt oxides was pronounced at the nanosized particles but not at the extended foil.

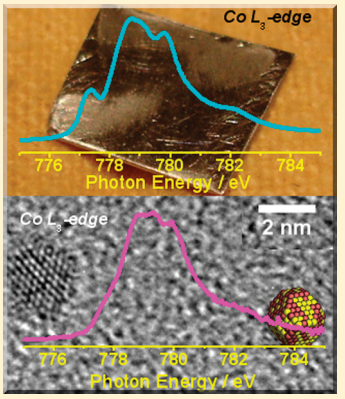

SECTION: Nanoparticles and Nanostructures

Intermetallic compounds and alloys play a key role in many technological areas because they often demonstrate distinctly different properties compared to the parent metals. Their surface structure, composition, and oxidation state are dynamic and not only depend on the intrinsic characteristics of the individual components, for example, surface energies and the strength of the intermetallic bonds, but can also be significantly influenced by the presence of adsorbents.[1−3] Typically, the alloy component that forms the strongest chemical bond with the adsorbent segregates toward the surface.[1] However, adsorption-driven surface segregation at the nanometer scale may differ from the bulk due to the high surface-to-volume ratio,[4] highlighting new routes in dynamical engineering of alloy surfaces for emerging nanotechnologies. Among others, Pt−Co nanoalloys are of large and growing interest because of their potential applications in fields such as magnetism[5] and (electro)catalysis.[6,7] In this work, the behavior of the polycrystalline PtCo foil and 3 nm PtCo nanoparticles (PtCo NPs) prepared by the low-energy cluster beam deposition (LECBD) technique was monitored in situ under 0.2 mbar of O_2 and H_2 by ambient pressure photoelectron (APPES) and near-edge X-ray absorption fine structure (NEXAFS) spectroscopies. Our results revealed extensive and reversible dealloying of PtCo in an oxidative atmosphere. The electronic structure and reducibility of the surface-segregated cobalt oxide are size-dependent. Surprisingly, the wurtzite cobaltous oxide phase (w-CoO), which is metastable in the bulk, is proven to be highly stable at the nanoscale.

Figure 1 shows the photoemission spectra of PtCo NPs and foil recorded in 0.2 mbar of O_2 and H_2 at 520 K. In H_2, the Pt $4f_{7/2}$ peak for both NPs and foil (Figure 1a) was found at 71.4 ± 0.1 eV, in agreement with literature values for PtCo alloys.[8,9] Annealing the NPs in O_2 does not influence the Pt 4f spectrum, in contrast to the PtCo foil, where the Pt 4f peak disappears (photoelectron kinetic energy (KE) of 1290 eV and information depth (ID) of ~5.5 nm).[10] Photoemission spectra over a wide energy range are composed only of cobalt and oxygen peaks, indicating extensive dealloying and Pt migration into the inner layers. The oxidation state of cobalt in the PtCo foil (Figure 1b, bottom spectra) switches from Co_3O_4 to metallic Co[11] in response to the oxygen chemical potential in the gas phase. In particular, in O_2, the Co $2p_{3/2}$ photoemission peak at 779.6 eV is accompanied by a weak, broad shakeup satellite structure, characteristic of the Co_3O_4 spinel phase.[12] When the gas atmosphere switches to H_2, the peak is shifted at 778.2 eV, and the satellite structure almost disappears, as expected for metallic cobalt (Co^0).[11] The modifications are rapid and reversible, as revealed by real time in situ photoelectron experiments (Figure S1, Supporting Information). In the case of PtCo NPs, in O_2, the Co $2p_{3/2}$ spectrum contains an intense shakeup structure characteristic

Received: March 8, 2011
Accepted: March 29, 2011
Published: April 04, 2011

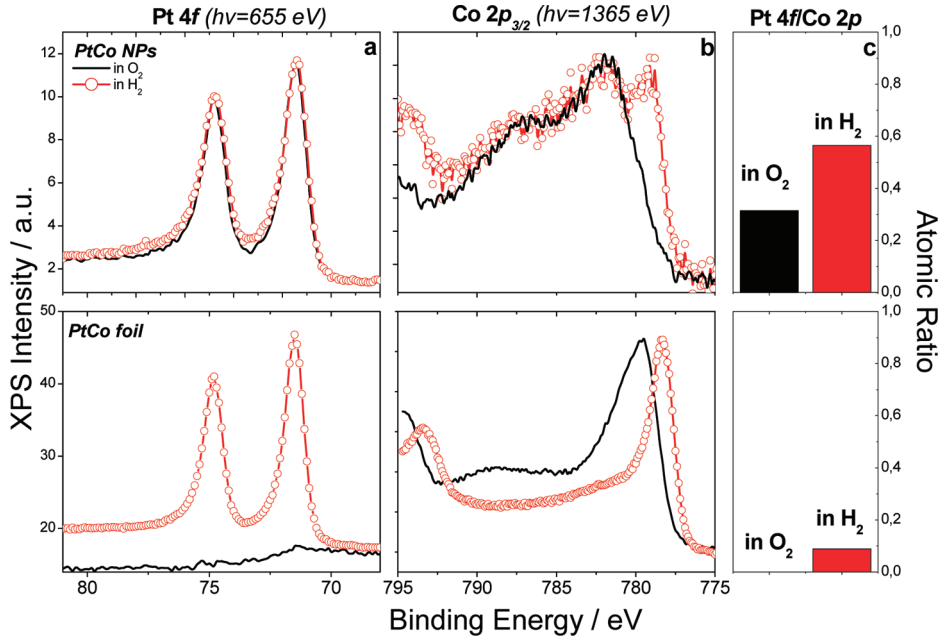

Figure 1. (a) The relative Pt 4f and (b) the Co $2p_{3/2}$ photoelectron peaks of 3 nm PtCo NPs (top) and the polycrystalline foil (bottom) recorded at 520 K in 0.2 mbar of O_2 (solid lines) and H_2 (open circles). The spectra are normalized in height to facilitate comparison. (c) The Pt 4f/Co 2p atomic ratio (photoelectron KE = 580 eV) calculated for NPs and foil samples under the same temperature and gas atmosphere conditions.

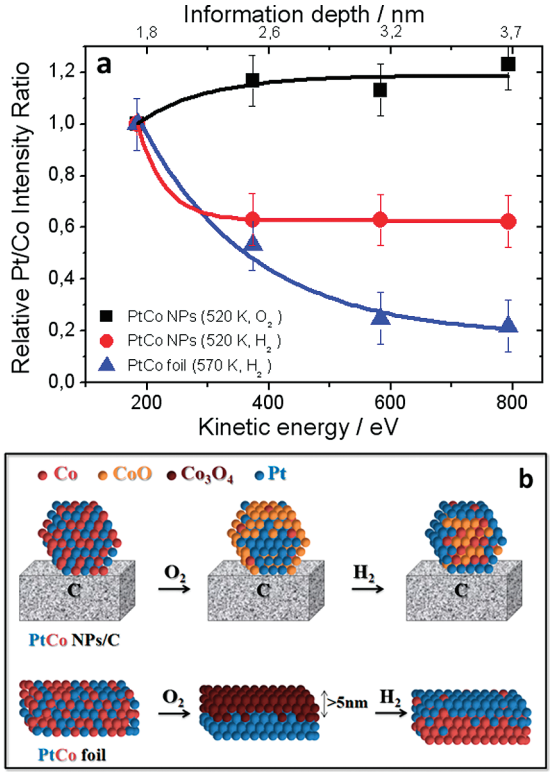

Figure 2. (a) The Pt/Co atomic ratio calculated from the Pt 4f and Co 2p photoelectron peaks as a function of the electron KE, measured at 520 K for PtCo NPs in O_2 and in H_2 and for the PtCo foil in H_2. On the upper *x*-axis, the estimated average ID for each electron KE is given. (b) Schematic model illustration of the proposed PtCo atom arrangement in NPs and foil under oxidative and reductive environments.

of CoO-like oxide formation.[11,12] In H_2, an additional component at 779.3 eV is attributed to reduced cobalt species, most probably in the metallic state.[11] However, the CoO-like oxide formed over NPs is significantly more difficult to reduce compared to the foil even at higher temperatures (as will be discussed in detail below). The Pt/Co atomic ratio (Figure 1c) increases in H_2 as compared to that in an O_2 atmosphere, clearly showing that reduction favors surface segregation of Pt.

The depth distribution of Pt and Co over the first few atomic layers was investigated by nondestructive depth profile measurements. The relative Pt 4f/Co 2p atomic ratios (details are given in section S2, Supporting Information) in different IDs are shown in Figure 2a. In H_2, the PtCo NPs and foil follow the same trend, that is, when deeper layers are probed, the Pt/Co intensity ratio decreases, indicating that Pt is preferentially localized on the surface and Co is in the subsurface region. In the case of NPs, the Pt/Co ratio stabilizes for KEs higher than 370 eV (ID $\approx$ 2.5 nm)[10] because, practically, the entire NP volume is probed. On the contrary, in an O_2 atmosphere, the inverse trend is observed, indicating the enrichment of cobalt (oxide) on a PtCo NP surface, in line with the results found for the PtCo foil (Figure 1). A schematic model of the surface arrangement of PtCo NPs and foil under oxidizing and reducing conditions is given in Figure 2b. In O_2, cobalt is oxidized to Co_3O_4 at the foil or to a CoO-like oxide at the NPs and encapsulates Pt. In H_2, cobalt oxides reduce to the metallic state at the foil or to a mixed CoO/Co state at the NPs, while Pt segregates back to the surface. Notably, modifying the conditions (e.g., temperature, Figure S3 Supporting Information) has a direct effect on the surface state, indicating the importance of the in situ approach for this study.

The "resistance" of the CoO-like oxide formed on NPs for further oxidation and reduction is rather surprising because CoO formed over the PtCo foil could be easily further oxidized to

dx.doi.org/10.1021/jz2003155 |J. Phys. Chem. Lett. 2011, 2, 900–904

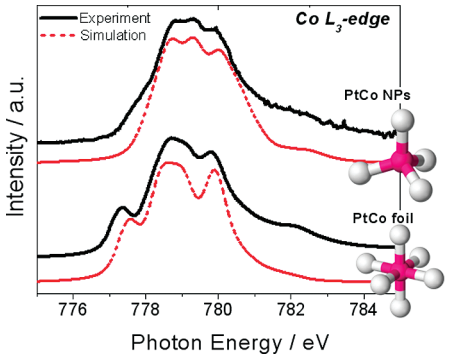

Figure 3. The experimental (black solid line) and theoretically simulated (red dashed line) Co L_3-edge absorption spectra of CoO-type oxides formed on the surface of NPs and foil PtCo alloys. Experimental data recording conditions: (i) NPs; 0.2 mbar of O_2 at 520 K; (ii) foil; preoxidized sample in 0.2 mbar of H_2 at 450 K. Charge-transfer parameters used for the calculations of theoretical spectra: (i) tetrahedrally coordinated Co^{2+}; $10D_q = -0.3$ eV, $D_t = -0.3$ eV, $D_s = 0$ eV; (ii) octahedrally coordinated Co^{2+}; $10D_q = 0.6$ eV, $\Delta = 5$ eV.

Co_3O_4 or reduced to Co. Theoretical simulation of the NEXAFS Co L_3-edge was used to compare the local environment and symmetry of cobalt ions in CoO-like oxides grown on PtCo NPs and foil. For that purpose, CoO oxide was stabilized on the PtCo foil surface by careful manipulation of pretreatment, temperature, and gas conditions. As depicted in Figure 3 the L_3-edge of CoO formed on NPs is reproduced by high-spin Co^{2+} tetrahedrally coordinated with four O^{2-} ions, as in hexagonal w-CoO.[13] In contrast, for the PtCo foil, the Co L_3-edge simulation indicates octahedrally coordinated Co^{2+}, as expected for cubic rocksalt bulk CoO (r-CoO).[12,13] These results are in agreement with our recent studies over monometallic 3.5 nm Co NPs,[14] which also showed formation of w-CoO (coexisting with the r-CoO). The high stability of w-CoO upon dealloying of the NPs is of particular interest because this phase is considered metastable in the bulk and is known to stabilize only in mixed cobalt oxides ($Zn_{1-x}Co_xO$)[15] or ultrathin epitaxial films.[16] Bulk-type Co_3O_4 formation is thermodynamically feasible under our conditions, as revealed by the results on the PtCo foil. Therefore, the stabilization of w-CoO on NPs is mainly kinetically controlled and not imposed by our pressure and temperature conditions. The same picture has been recently found during preparation of pure cobalt oxide nanocrystals (>20 nm).[13] It was shown that kinetic control conditions (rapid heating at high temperatures) yield tetrahedral w-CoO, while thermodynamic control conditions (prolonged heating at lower temperatures) produce octahedral r-CoO.[13] Due to the limited size (3 nm) of PtCo NPs, the interface between the Pt atoms and the cobalt oxide overlayer dominates the oxide structure. Subsurface Pt imposes severe constrains on the atomic arrangement of the cobalt overlayer, stabilizing the metastable w-CoO phase. These constrains might be related to epitaxial strain and/or electronic interaction (charge transfer)[17] and may significantly modify the physicochemical properties and the reactivity of the nanosized cobalt oxide as compared to the bulk.[17,18] On the other hand, in the extended alloy, Pt atoms migrate far from the near-surface region (>5 nm), and therefore, the oxide/metal interface is less influential on the cobalt oxide structure. Consequently, the thermodynamically favorable spinel Co_3O_4 is formed. Stabilization of novel oxide nanostructres is a well-established effect in

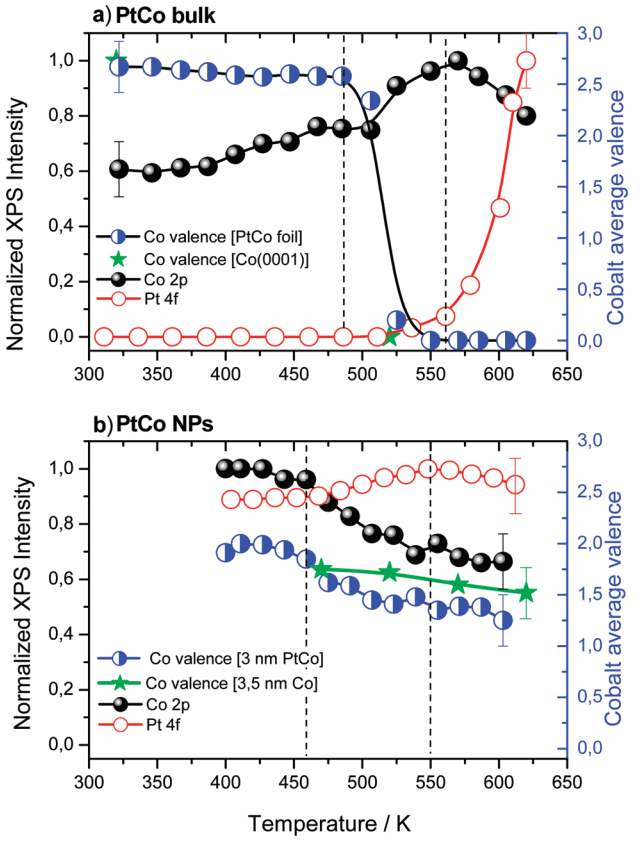

Figure 4. Temperature-programmed reduction (temperature rate: 5 K min^{-1}) of preoxidized (a) polycrystalline PtCo foil and (b) 3 nm PtCo NPs recorded in situ and in real time under [(open circles) Pt 4f intensity; (closed circles) Co 2p intensity; (demi-filled circles) average cobalt valency]. The star points represent the average cobalt valency of preoxidized pure 3.5 nm Co NPs and Co(0001) single-crystalline surfaces under identical conditions, recorded as a reference.

low-dimensional oxides grown on metal supports.[17] Typically, due to the differences in the lattice constants, the metal support imposes severe constraints on the atomic arrangement of the oxide overlayer, which is of course more influential at their interface. This induces major perturbations in the structure and the electronic properties of the nanosized oxides but also produces an internal elastic strain. As has been previously shown (see ref 17 and references therein), these factors affect the reactivity of the nanostructured oxides as compared to their bulk counterparts. We propose that the stabilization of the ultrathin w-CoO overlayer around the Pt metal core, following the dealloying of PtCo NPs, is the nanosized equivalent of these well-defined phenomena.

The addition of Pt promoters is often employed in Co-based catalysts in order to facilitate the reduction of cobalt oxides.[5] Here, the reduction of the PtCo alloys is monitored in situ and in real time upon annealing preoxidized samples in a H_2 atmosphere. Experiments were performed on both nanosized and extended alloys, while reference spectra on pure 3.5 nm Co NPs and Co(0001) single crystals were recorded at some characteristic temperatures. The initially oxidized surfaces were prepared by treating the samples in 0.2 mbar of O_2 and at 670 K (570 K for NPs) for 10 min. Figure 4 shows the intensity evolution of both the Pt 4f and Co 2p photoelectron peaks (referring to the maximum recorded intensity) for extended (Figure 4a) and

dx.doi.org/10.1021/jz2003155 |J. Phys. Chem. Lett. 2011, 2, 900–904

nanosized (Figure 4b) alloys as a function of temperature. The average Co valency calculated by deconvolution of the overall Co 2p peak to metallic and oxide components is also included.

We first turn our attention to the PtCo foil where three distinct temperature regions are evident, as follows: (i) The first is an initial low-temperature region (T < 490 K) where the Co oxidation state and Pt signal remain stable but the Co 2p signal slightly increases. As supported by the changes in C 1s and O 1s peaks, this increase is due to the removal/oxidation of residual carbon and hydroxyl species that are adsorbed at low temperatures on the Co_3O_4 surface and attenuate the Co 2p signal. (ii) Second is an intermediate temperature region (490−560 K), where the Co signal increase is steeper, followed by rapid reduction of cobalt oxide and a slight increase of Pt signal. Please note that cobalt reduction comes first and is followed by the appearance of a Pt signal, and (iii) a third is a high-temperature region (T > 560 K), where the Co signal decreases and the Pt 4f intensity sharply increases. In this region, metallic Co is diluted in the subsurface, while Pt atoms segregate at the top surface layers. Reference experiments performed on a Co(0001) crystal (indicated by stars in the graph) gave fairly similar results, indicating no significant promotion effect of Pt in the reduction of Co for the bulk sample (foil). This is also reflected by the fact that the Pt signal appears shortly after cobalt has reverted to the metallic state.

The changes induced by annealing the PtCo NPs are more subtle but nevertheless detectable. Up to 460 K, the Pt and Co intensities, as well as the mean Co valency, remain practically stable. Intensity changes become apparent upon further heating up to 550 K; the Pt intensity increases, while the Co intensity and valency decrease. Finally, at temperatures up to 620 K, the Pt and Co intensities as well as the Co valency remain approximately the same. Annealing at temperatures higher than 620 K induces significant decrease of both Pt 4f and Co 2p signals, indicating that particle agglomeration and/or diffusion become significant, and therefore, these results are not presented. For comparison, the Co valency of a 3.5 nm Co NP pretreated under the same conditions is included in the graph. An increase of the reduction degree of PtCo compared to monometallic Co NPs (indicated by stars in the graph) is clearly observed. It can be also seen by comparison of Figure 4a and b that in the critical temperature window of cobalt oxide reduction (470−550 K), nanosized and extended PtCo alloys show different trends. On the foil, Pt segregation starts right after cobalt oxide reduction, while for the NPs, cobalt reduction is followed by progressive Pt segregation. Therefore, one can assume that Pt and Co in the NPs are in close interaction, and Pt plays a role in the reduction of the cobalt oxide formed on the NPs. This can also explain why the reduction of bimetallic PtCo NPs is much more efficient at the same conditions compared to that of monometallic cobalt NPs with similar size (Figure 4b). On the basis of literature data,[19] Pt is a very efficient catalyst for hydrogen adsorption and dissociation that can provide highly reactive atomic hydrogen, which facilitates cobalt reduction.

Summarizing, our results indicated rapid and extended dealloying of PtCo in response to the surrounding gas atmosphere. The electronic structure of the segregated cobalt oxide in the nanoscale is markedly different from the corresponding bulk material. Kinetic limitations in the nanometer size range lead to high chemical stability of (metastable in the bulk) w-CoO. This work provides insights into the PtCo nanoalloys' surface chemistry, which is crucial to rationalize their performance in catalysis and magnetism. Our results also propose a general strategy towards stabilization of metastable oxide structures in the nanoscale through the deliberate adsorbed-driven surface segregation over bimetallic nanoalloys.

EXPERIMENTAL SECTION

PtCo NPs (3.00 ± 0.22 nm) deposited on a Si substrate covered by a 10 nm thick amorphous carbon layer were prepared following the LECBD technique[20] (details in Supporting Information section S4). The PtCo clusters are in the chemically disordered A1 fcc phase and have a perfect truncated octahedron shape.[21] The size stability in our conditions was confirmed by APPES (Supporting Information Figure S5). The polycrystalline PtCo foil was prepared by conventional metallurgy. APPES and NEXAFS measurements were performed at the ISISS beamline at the BESSY synchrotron facility at the Helmholtz Zentrum Berlin.[22] The $L_{2,3}$-edge absorption spectra were simulated based on the charge-transfer multiplet (CTM) approach[23] using the CTM4XAS vs3.1 program.[24]

ASSOCIATED CONTENT

Supporting Information. Real time experiments in the PtCo foil, details for the calculation of the relative Pt 4f/Co 2p atomic ratios at different information depths, Co L_3 NEXAFS spectra of the PtCo foil at different temperatures, and details of the preparation and stability of the PtCo nanoparticles. This material is available free of charge via the Internet at http://pubs.acs.org.

AUTHOR INFORMATION

Corresponding Author
*E-mail:spiros.zafeiratos@unistra.fr.

ACKNOWLEDGMENT

We acknowledge useful discussions with E. Savinova and F. Garin. Financial support from FP7-FCH-JU-2008-1-CP: ROBANODE, DEMMEA, IRAFC projects, BESSY II EUSA program, French ANR/PNANO-07 (ETNAA) project, and COST actions MP0903 "Nanoalloys as Advanced Materials: From Structure to Properties and Applications" are gratefully acknowledged. The authors would also like to thank the BESSY II staff for their help in carrying out the experiments, in particular, R. Follath for implementation of the continuous monochromator driving mode for XAS measurements.

REFERENCES

(1) Tao, F.; Grass, M. E.; Zhang, Y.; Butcher, D. R.; Renzas, J. R.; Liu, Z.; Chung, J. Y.; Mun, B. S.; Salmeron, M.; Somorjai, G. A. Reaction-Driven Restructuring of Rh−Pd and Pt−Pd Core−Shell Nanoparticles. *Science* **2008**, *322*, 932–934.

(2) Piccinin, S.; Zafeiratos, S.; Stampfl, C.; Hansen, T. W.; Haevecker, M.; Teschner, D.; Bukhtiyarov, V. I.; Girgsdies, F.; Knop-Gericke, A.; Schloegl, R.; et al. Alloy Catalyst in a Reactive Environment: The Example of Ag−Cu Particles for Ethylene Epoxidation. *Phys. Rev. Lett.* **2010**, *104*, 035503.

(3) Kitchin, J. R.; Reuter, K.; Scheffler, M. Alloy Surface Segregation in Reactive Environments: First-Principles Atomistic Thermodynamics Study of $Ag_3Pd(111)$ in Oxygen Atmospheres. *Phys. Rev. B* **2008**, *77*, 075437.

(4) Wang, C. X.; Yang, G. W. Thermodynamics of Metastable Phase Nucleation at the Nanoscale. *Mater. Sci. Eng. R* **2005**, *49*, 157–202.
(5) Ferrando, R.; Jellinek, J.; Johnston, R. L. Nanoalloys: From Theory to Applications of Alloy Clusters and Nanoparticles. *Chem. Rev.* **2008**, *108*, 845–910.
(6) Stamenkovic, V. R.; Mun, B. S.; Arenz, M.; Mayrhofer, K. J. J.; Lucas, C. A.; Wang, G. F.; Ross, P. N.; Markovic, N. M. Trends in Electrocatalysis on Extended and Nanoscale Pt−Bimetallic Alloy Surfaces. *Nat. Mater.* **2007**, *6*, 241–247.
(7) Chu, W.; Chernavskii, P. A.; Gengembre, L.; Pankina, G. A.; Fongarland, P.; Khodakov., A. Y. Cobalt Species in Promoted Cobalt Alumina-Supported Fischer−Tropsch Catalysts. *J. Catal.* **2007**, *252*, 215–230.
(8) Wakisaka, M.; Mitsui, S.; Hirose, Y.; Kawashima, K.; Uchida, H.; Watanabe, M. Electronic Structures of Pt−Co and Pt−Ru Alloys for Co-Tolerant Anode Catalysts in Polymer Electrolyte Fuel Cells Studied by EC-XPS. *J. Phys. Chem. B* **2006**, *110*, 23489–23496.
(9) Tuaillon-Combes, J.; Bernstein, E.; Boisron, O.; Melinon, P. Alloying Effect in CoPt Nanoparticles Probed by X-ray Photoemission Spectroscopy: Validity of the Bulk Phase Diagram. *J. Phys. Chem. C* **2010**, *114*, 13168–13175.
(10) Seah, M.P. In *Practical Surface Analysis*; Briggs, D., Seah, M. P., Eds.; Wiley & Sons: Chichester, U.K., 1992; Vol 1, p 209.
(11) Zafeiratos, S.; Dintzer, T.; Teschner, D.; Blume, R.; Hävecker, M.; Knop-Gericke, A.; Schlögl, R. Methanol Oxidation Over Model Cobalt Catalysts: Influence of the Cobalt Oxidation State on the Reactivity. *J. Catal.* **2010**, *269*, 309–317.
(12) Vaz, C. A. F.; Prabhakaran, D.; Altman, E. I.; Henrich, V. E. Experimental Study of the Interfacial Cobalt Oxide in Co_3O_4/α-Al_2O_3-(0001) Epitaxial Films. *Phys. Rev. B* **2009**, *80*, 155457.
(13) Nam, K. M.; Shim, J. H.; Han, D. W.; Kwon, H. S.; Kang, Y. M.; Li, Y.; Song, H; Seo, W. S.; Park, J. T. Syntheses and Characterization of Wurtzite CoO, Rocksalt CoO, and Spinel Co_3O_4 Nanocrystals: Their Interconyersion and Tuning of Phase and Morphology. *Chem. Mater.* **2010**, *22*, 4446–4454.
(14) Papaefthimiou, V.; Dintzer, T.; Dupuis, V.; Tamion, A.; Tournus, F.; Hillion, A.; Teschner, D.; Hävecker, M.; Knop-Gericke, A.; Schlögl, R.; et al. Nontrivial Redox Behavior of Nanosized Cobalt: New Insights from Ambient Pressure X-ray Photoelectron and Absorption Spectroscopies. *ACS Nano* **2011**, *5*, 2182–2190.
(15) Venkatesan, M.; Fitzgerald, C. B.; Lunney, J. G.; Coey, J. M. D. Anisotropic Ferromagnetism in Substituted Zinc Oxide. *Phys. Rev. Lett.* **2004**, *93*, 177206.
(16) Meyer, W.; Hock, D.; Biedermann, K.; Gubo, M.; Müller, S.; Hammer, L.; Heinz, K. Coexistence of Rocksalt and Wurtzite Structure in Nanosized CoO Films. *Phys. Rev. Lett.* **2008**, *101*, 016103.
(17) Netzer, F. P.; Allegretti, F.; Surnev, S. Low-Dimensional Oxide Nanostructures on Metals: Hybrid Systems with Novel Properties *J. Vac. Sci. Technol., B* **2010**, *28*, 1–16.
(18) Grass, M. E.; Zhang, Y.; Butcher, D. R.; Park, J. Y.; Li, Y.; Bluhm, H.; Bratlie, K. M.; Zhang, T.; Somorjai, G. A. A Reactive Oxide Overlayer on Rhodium Nanoparticles during CO Oxidation and Its Size Dependence Studied by In Situ Ambient-Pressure X-ray Photoelectron Spectroscopy. *Angew. Chem., Int. Ed.* **2008**, *47*, 8893–8896.
(19) Borgna, A.; Anderson, B. G.; Saib, A. M.; Bluhm, H.; Havecker, M.; Knop-Gericke, A.; Kuiper, A. E. T.; Tamminga, Y.; Niemantsverdriet, J. W. Pt-CO/SiO_2 Bimetallic Planar Model Catalysts for Selective Hydrogenation of Crotonaldehyde. *J. Phys. Chem. B* **2004**, *108*, 17905–17914.
(20) Tamion, A.; Raufast, C.; Bonet, E.; Dupuis, V.; Fournier, T.; Crozes, T.; Bernstein, E.; Wernsdorfer, W. Magnetization Reversal of a Single Cobalt Cluster Using a RF Field Pulse. *J. Magn. Magn. Mater.* **2010**, *622*, 1315–1318.
(21) Tournus, F.; Rohart, S.; Dupuis, V. Magnetic Anisotropy Dispersion in CoPt Nanoparticles: An Evaluation Using the Neel Model. *IEEE Trans. Magn.* **2008**, *44*, 3201–3204.
(22) Knop-Gericke, A.; Kleimenov, E.; Hävecker, M.; Blume, R.; Teschner, D.; Zafeiratos, S.; Schlögl, R.; Bukhtiyarov, V. I.; Kaichev, V. V.; Prosvirin, I. P.; et al. X-ray Photoelectron Spectroscopy for Investigation of Heterogeneous Catalytic Processes. *Adv. Catal.* **2009**, *52*, 213–272.
(23) de Groot, F. High-Resolution X-ray Emission and X-ray Absorption Spectroscopy. *Chem. Rev.* **2001**, *101*, 1779–1808.
(24) Stavitski, E.; de Groot, F. M. F. The CTM4XAS Program for EELS and XAS Spectral Shape Analysis of Transition Metal L Edges. *Micron* **2010**, *41*, 687–694.